JTTEE 3:57-62

Hot Isostatic Pressing of Plasma Sprayed Ni-Base Alloys

K.A. Khor and N.L. Loh

This article reports the effects of hot isostatic pressing (HIPing) on the microstructure and properties of plasma sprayed Ni-based alloy coatings. Hot isostatic pressing was used as a post-spray treatment on plasma sprayed Ni-5Al, Ni-20Al, and NiCrAl coatings. The aim was to densify the coatings and modify physical properties such as strength, amount of porosity, and hardness. The coatings were HIPed at 750 to 950 °C at pressures of 50 to 200 MPa and held for 1 h. The treated coatings were examined by optical microscopy and scanning electron microscopy (SEM). Coating porosity was determined using a combination of an image analyzer and SEM. Near-zero porosity levels could be obtained, and HIP treatment at increasing temperatures and pressures changed the microstructure and increased the microhardness of the coatings. Mechanical testing of the coatings was performed on a Dynamic Mechanical Analyzer (DMA) from ambient to ~1000 °C. The results showed that the elastic modulus of HIPed coatings was greater than as-sprayed coatings up to ~750 °C. These changes can be related to plastic flow, interlamellar diffusion, and creep that occur at increased temperatures and pressures.

1. Introduction

PLASMA-SPRAYED nickel-based coatings such as Ni-5Al, Ni-20Al, NiCrAl, and the MCrAlY series have been applied on various metal surfaces as intermediate bond coats for thermal barrier coatings (TBCs).[1] The Ni-Al coatings are known for their excellent bond strengths,[2,3] and it has been hypothesized that the nickel and aluminum combine in an exothermic reaction, leading to the partial oxidation of the components. Another study, however, suggests that the presence of aluminum enhances coating integrity by deoxidizing the molten Ni-Al droplets to produce nonporous splats with a higher degree of contact as a result of reduced interlamellar porosity.[4,5] This topic is still a point of dispute within the thermal spray community. The sprayed layers consist of an inhomogeneous combination of various compounds that form in the flame. Knotek et al. reported the formation of metallic nickel, aluminum, Ni_3Al, and NiO in Ni-5Al coatings.[6] Coatings of Ni-20Al consist of the same phases as well as some γ-Al_2O_3 and traces of NiAl.[7] Sheppard found NiAl, Ni_3Al, NiO, and $NiAl_2O_4$ in the coatings.[8] Cheang, however, did not detect any nickel aluminides in plasma-sprayed Ni-Al; only Ni, NiO, and traces of γ-Al_2O_3.[4] A drawback of nickel aluminide is its inherent brittleness. The addition of chromium to nickel aluminide to form NiCrAl results in an alloy with substantial tensile ductility that still retains attractive elevated temperature properties, especially in the presence of hot corrosive gases.

One inherent aspect of plasma-sprayed coatings is porosity, which ranges from ~1 to 30% depending on the method of measuring porosity, powder characteristics, and spraying conditions. A study on the pore size distribution of Ni-Al plasma-sprayed coatings using mercury intrusion porosimetry (MIP) and SEM was consistent with a two-level porosity model consisting of isolated pores in the size range ~1 to 10 μm interconnected by a network of ~0.1 μm planar pores.[9] Another study on the structure of alumina coatings using copper electroplating indicated that the bonding at the interfaces of the quenched splats was rather limited.[10] The maximum mean bond rate was reported to be ~32%. The real area of contact between individual lamellae within the coating and between lamellae was much less than the apparent area because of absorbed and entrapped gas, oxide films, or other contamination.[11] This could help explain the lower mechanical strength of the coatings compared to the bulk material. Post-spray treatment such as laser glazing or hot isostatic pressing is therefore necessary to reduce porosity levels and improve coating strength and hardness.

In the HIP process, pressure and temperature are applied simultaneously to the workpiece. The pressurization medium is in the form of a gas (argon, nitrogen, and oxygen), and the pressure applied is equal in all directions (isostatic). The part to be pressed must have a gas-tight skin or must be "canned," because no consolidation takes place if gas can penetrate through the surface. HIPing has been used in the consolidation of both metal and ceramic powders into near-net shapes and in the removal of porosity in metal castings and weldments. The application of HIP to the densification of plasma-sprayed coatings has been studied on several ceramics (ZrO_2-7 wt% Y_2O_3, CaO-stabilized ZrO_2, and alumina) and cermet (WC/Co) coatings.[12-14] These studies showed that porosity levels were considerably reduced and other physical properties (hardness and tensile strength) were improved.

The present study investigates the use of HIP as a post-spray treatment for plasma-sprayed Ni-5Al, Ni-20Al, and NiCrAl coatings. Optical and scanning electron microscopy were used to examine changes in the microstructure of the coatings after HIP. Porosity measurements were performed with an advanced image analyzer on scanned images exported from a SEM. The measurement was achieved on polished cross sections of the coatings. The microhardness measurements were taken along the traverse section of the polished specimens.

Key Words: hot isostatic pressing, mechanical properties, porosity, post-spray treatment

K.A. Khor and **N.L. Loh**, School of Mechanical & Production Engineering, Nanyang Technological University, Singapore 2263, Singapore.

Table 1 Spray parameters of Ni-5Al, NI-20Al, and NiCrAl coatings

Powder type	Primary arc gas pressure, psi	Secondary arc gas pressure, psi	Feed rate, rpm	Current, A
Ni-5Al	50	100	4.1	800
Ni-20Al	50	...	5.5	800
NiCrAl	50	100	4	800

Note: 1 psi = 6.89 kN/m^2.

Table 2 Parameters used for HIP cycles

HIP cycle	Temperature, °C	Pressure, MPa	Holding time, min
1	750	200	60
2	800	50	30
3	800	105	60
4	850	105	60
5	850	200	60
6	900	105	60
7	900	200	60
8	950	50	60

2. Experimental Procedure

Prealloyed Ni-5Al (AI 1037), NiCrAl (AI 1047), and composite Ni-20Al (AI 1404) powders were used as feedstock. The composition of the NiCrAl alloy was (wt%) 4.5 to 7.5% Al, 15.5 to 21.5% Cr, bal Ni. The substrates were medium-carbon steel plate (50 × 100 × 2.5 mm), which had been grit blasted. The powders were plasma sprayed using a 40-kW plasma spray system from Miller Thermal Inc. Argon (primary) and helium (secondary) were used as the plasma forming gas. Table 1 lists the spray parameters used for the above powders. Small pieces of the coatings, about 200 mm^2 in area, were sectioned using a diamond blade, cleaned, and packed in a mild steel capsule with ZrO_2-7 wt% Y_2O_3 (particle size range 45 to 75 μm) as the packing powder. A wire gauze was placed at the top of the can for improved sealing. The capsule lid was arc welded to the capsule after degassing was completed (vacuum level of ~2×10^{-2} mbar). The HIP equipment used was the O_2 System 5X from Kobelco. A molybdenum furnace was used for heating, and argon gas was used as the pressure transmitting medium. Table 2 lists the parameters used in the HIP cycles.

The HIP runs identified as HIP 2 to 4 do not contain the Ni-20Al coating, and runs HIP 2 and 3 do not contain the NiCrAl coating. Microhardness measurements (Vickers 300-g load) of the HIPed specimens were obtained using the Matsuzawa DMH-1. The porosity was measured using a combination of the Cambridge S360 SEM or optical microscope and the Quantimet Q570 image analyzer. In the former arrangement, the high-magnification image obtained in the SEM was transferred to the image analyzer via an image transfer interface between the SEM and the image analyzer. Subsequently, the image was further processed using the morphological functions within the image analyzer.

The dynamic mechanical analyzer used in this study was the Perkin Elmer Series 7 DMA that is capable of stress scan, temperature scan, and frequency scan analyses. It makes use of a three-point bending jig to determine the mechanical properties of the coatings from ambient to ~1000 °C. The specimen size was approximately 7.0 × 3.0 × 0.15 mm. The coating thickness (y) required for DMA was determined by the following relationship:

$$y^2 = 3Px/2zs$$

where P is the bending load, x is the width of the holder, mm; z is the depth of the coating, mm; and s is the required dynamic stress, MPa.

A predetermined stress of 40 MPa was loaded dynamically onto the sample at a frequency of 1 Hz. The cyclic load was applied in a sine wave manner. The heating rate was fixed at 10 °C/min. The results from the DMA reveal the dynamic properties such as storage and loss modulus. Only the Ni-5Al coatings were tested in this fashion.

3. Results and Discussion

3.1 *Microstructure*

Figure 1 shows the polished cross sections of as-sprayed Ni-5Al, Ni-20Al, and NiCrAl coatings, respectively. Evidence of oxidation can be observed in the form of oxide stringers. Pores are also evident, in particular around the oxide inclusions and unmelted or partially melted particles. On the other hand, the polished cross sections of HIPed coatings in Fig. 2(a through c) show some changes in the microstructures. The oxide stringers appeared to be thin and in some cases more linear due to increased stress and high-temperature (enough for some plastic deformation to occur) effects. The pores observed in the as-sprayed coatings have been reduced significantly. An additional feature observed predominantly in HIPed Ni-20Al coatings is the breakup of the oxides into smaller fragments. Evidence of this phenomenon is more marked at higher pressures (~200 MPa). Another feature more noted in the Ni-20Al coatings is the increase in the concentration of oxides at the top layer (~10 to 20 μm) of the coating (Fig. 3). One likely cause of this is residue air that remained after evacuation of the steel can for HIP, although the can had been evacuated to 1×10^{-2} mbar. The HIP sample treated at 750 °C did not exhibit such a marked increase in oxides at the top layer.

3.2 *Microhardness Measurements*

Table 3 presents the average Vickers hardness (300-g load) for each coating. Each hardness value in the table is an average of 20 readings. Figure 4 shows the percentage increase in hardness for some of the HIPed coatings. The Ni-20Al coatings exhibited the most significant increase in hardness (99% max) of

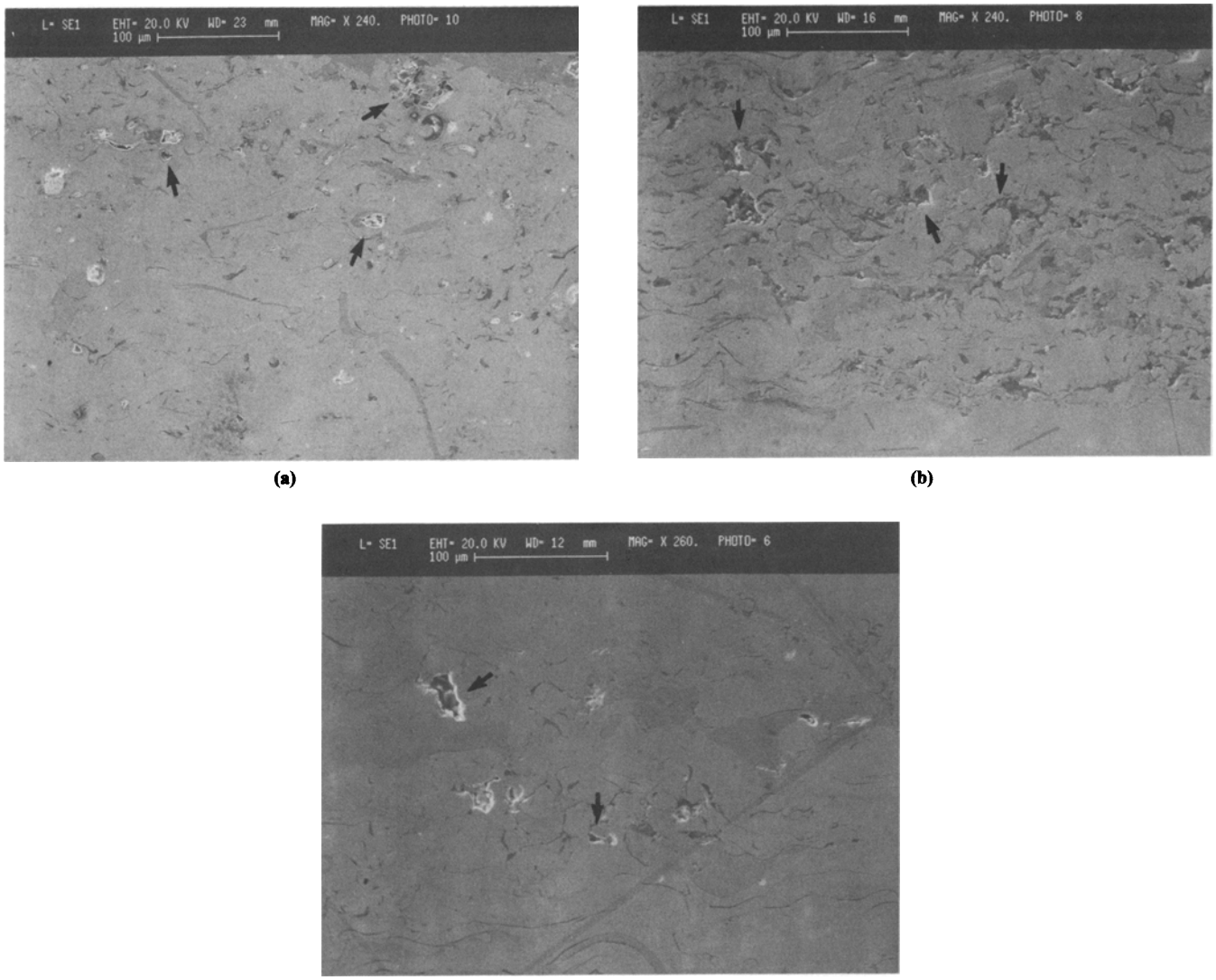

Fig. 1 Microstructure of as-sprayed Ni-based coatings (arrows refer to pores) **(a)** As-sprayed Ni-5Al coating **(b)** As-sprayed Ni-20Al coating **(c)** As-sprayed NiCrAl coating

Table 3 Average Vickers hardness measurement for each coating

Specimen No.	Vickers hardness, Ni-5Al	Ni-20Al	NiCrAl
As sprayed	139.1	203.4	245.5
HIP 1	138.3	241.6	255.2
HIP 2	159.6	...	...
HIP 3	145.2	...	...
HIP 4	143.8	...	274.2
HIP 5	182.3	361.8	323.9
HIP 6	170.1	383.8	299.5
HIP 7	180.2	405.1	331.2
HIP 8	205.9	363.3	350.3

the coatings. Part of this hardness increase is attributable to the increase in oxide content discussed in the previous section. On the other hand, the Ni-5Al coating showed a maximum increase of ~47% after HIP, whereas the NiCrAl coatings exhibited a maximum increase of ~59%. Figure 4 also shows that, for the Ni-20Al coatings, the hardness increase corresponds to the use of pressures that were greater than 100 MPa (e.g. samples HIP 6 and 7). On the other hand, the hardness of the Ni-5Al and NiCrAl coatings improved significantly at temperatures above 900 °C (HIP 8).

3.3 *Porosity Measurement*

Table 4 lists the porosity of the coatings measured by the SEM/image analyzer technique. Each porosity measurement was obtained from an average of six fields of view. Both Ni-5Al and NiCrAl coatings (HIP 8) exhibited the highest reduction in porosity (~90%). At 750 °C and 200 MPa, Ni-5Al exhibits the largest reduction in porosity, whereas the NiCrAl material responded well to higher temperature (950 °C). Note that the reduction in porosity in the Ni-20Al coatings is lower and is

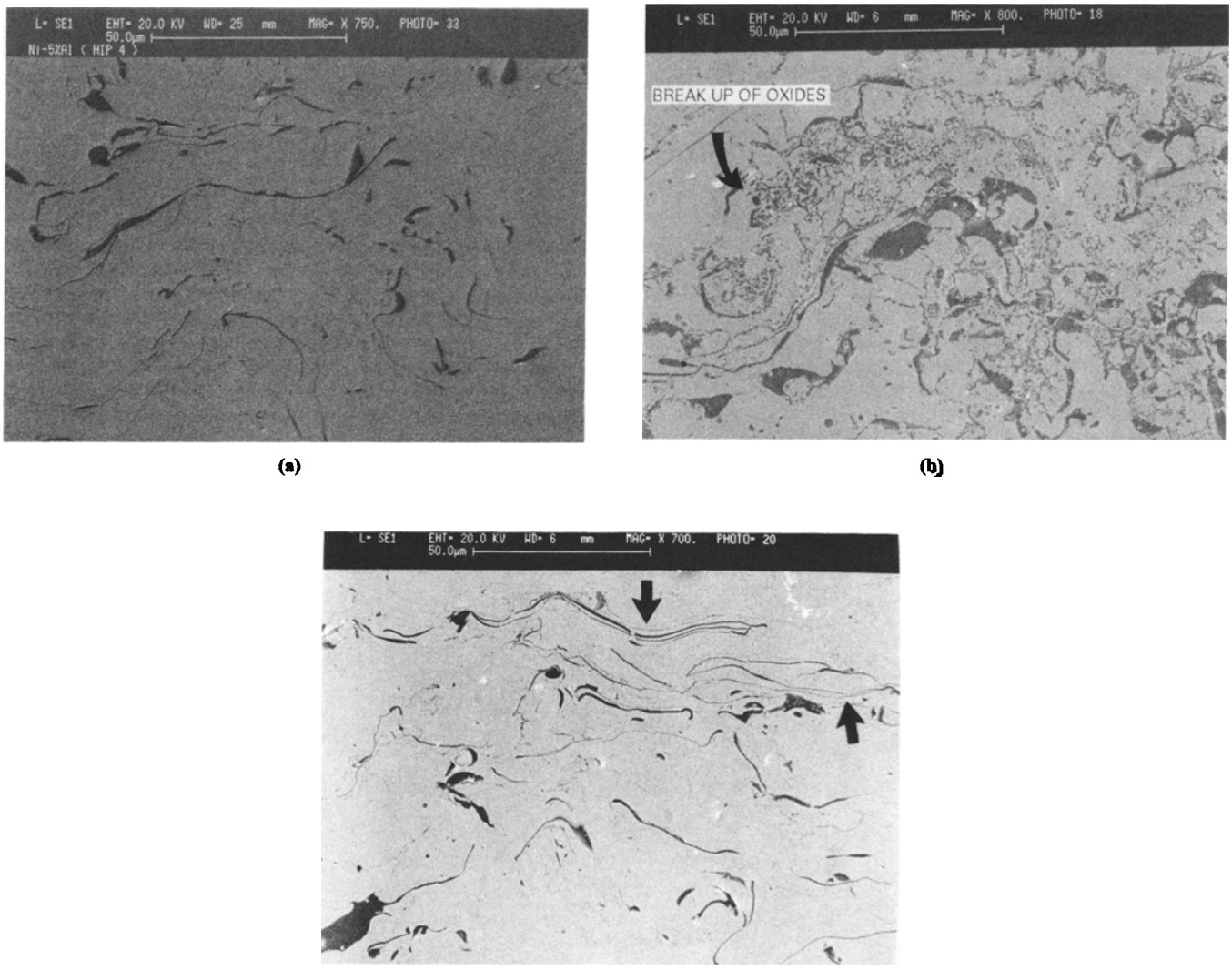

Fig. 2 SEM micrograph of polished cross section of HIPed Ni-based coatings **(a)** HIPed Ni-5Al **(b)** HIPed Ni-20Al **(c)** HIPed NiCrAl (arrows refer to oxide stringers that are more linear than before)

probably due to the difficulty in closing the pores around the oxides, as there are more oxides in the Ni-20Al coatings. In the Ni-5Al and NiCrAl coatings, where there is a relatively lower percentage of oxides, the pores exist mainly between the lamellae and around some unmelted and partially melted particles. These pores could be closed with relative ease at high temperatures and pressures compared to pores around the oxide inclusions and stringers, because there would not be any mismatch in the coefficient of thermal expansion and other surface properties.

3.5 *Mechanical Properties*

The DMA result shows that the HIPed Ni-5Al coating exhibits a Young's modulus of ~102 GPa. This value is significantly higher than the modulus of the as-sprayed coating, which is ~58 GPa. As the temperature increases, the modulus of the HIP specimen dropped progressively until ~740 °C, where it reaches the same level as the as-sprayed coating (Fig. 5). The difference in Young's modulus of the HIPed coating and the as-sprayed coating is most marked from ambient to ~500 °C. The increase in the modulus of the as-sprayed coating at 450 to 500 °C is due

Table 4 Porosity level of as-sprayed and HIPed coatings

Specimen	Porosity, %	Reduction in porosity, %
As-sprayed Ni-5Al	1.6	...
Ni-5Al (HIP 1)	0.32	80
Ni-5Al (HIP 8)	0.17	89.4
As-sprayed Ni-20Al	2.3	...
Ni-20Al (HIP 1)	0.84	63.5
Ni-20Al (HIP 8)	0.44	80.9
As-sprayed NiCrAl	1.2	...
NiCrAl (HIP 1)	0.5	58.3
NiCrAl (HIP 8)	0.12	90

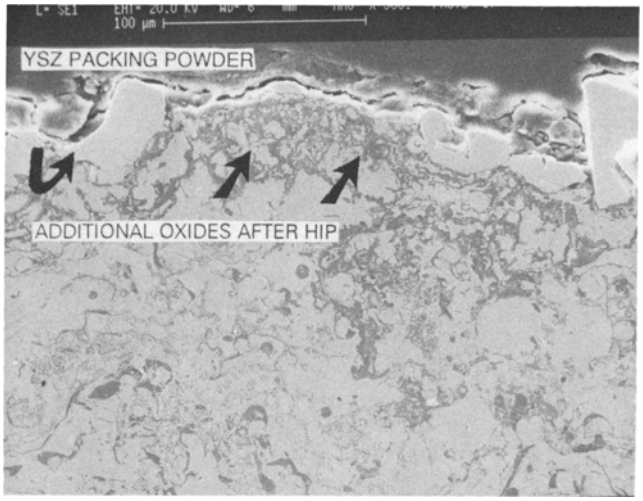

Fig. 3 Top layer of plasma-sprayed Ni-20Al coating after HIP showing the increased concentration of oxides

partly to the heat applied, which causes plastic flow, and partly to the closing of the interplanar pores. A slight increase in oxide content could also have contributed to this phenomenon.

HIP is a complex process, and several attempts have been made to model this process to predict densification rates and the dominant deformation mechanism for various combinations of time, temperature, and pressure. Plastic yielding, brought about by high pressures, caused the grains to yield and deform plastically, closing the pores. Increased temperature, together with the stress field applied, caused interlamellar diffusion such that material diffuses from areas between particles to the voids, enabling the lamellae to move closer together and consequently close the pores. However, according to Helle et al., if the holding time is sufficiently long, grain growth may occur and isolate pores.[15] This will suppress the diffusive mechanism because the pores no longer lie in the grain boundaries.

Coble creep and Nabarro-Herring creep are other possible mechanisms that contribute to the reduction of pores, but these phenomena come into effect at temperatures and pressures above the effective range for plastic yielding and interlamellar diffusion.[16] The HIP maps for Ni_3Al and Ni_3Al alloys drawn by Wright et al.,[17] based on a computer simulation program and compared to actual HIP experiments, suggest that, at a HIP condition of 850 °C and 207 MPa (similar to HIP 5), the majority of the densification occurs early due to the large initial contact, and full densification could be accomplished in ~600 s. The simulation results predicted the densification rate to be strongly dependent on temperature.[17] Hence, satisfactory densification of plasma-sprayed Ni-based coatings could actually be performed in a shorter time than that used in the present study (3600 s).

4. Conclusion

Evaluation of HIPed plasma sprayed Ni-based coatings has shown significant reduction in porosity level with an accompanying increase in hardness. These effects were more apparent at higher HIP pressures. The change in microstructure was in the

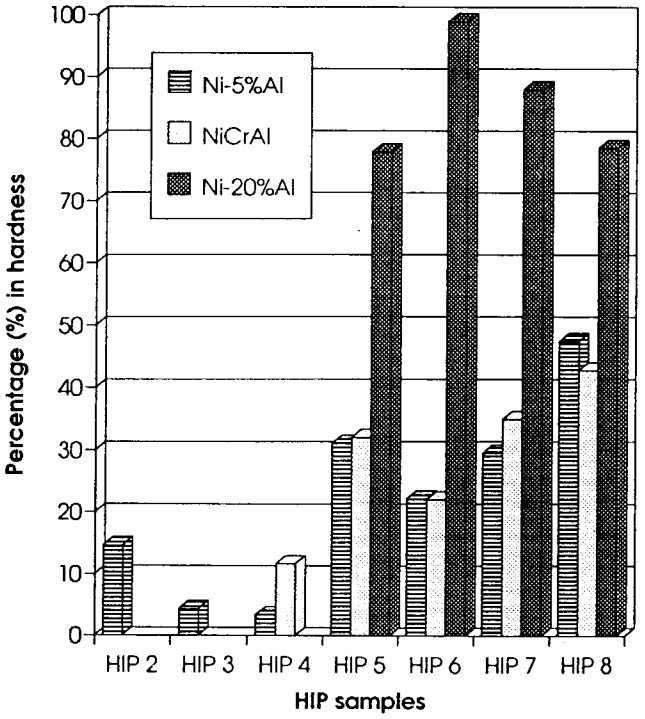

Fig. 4 Percentage increase in hardness for HIP samples

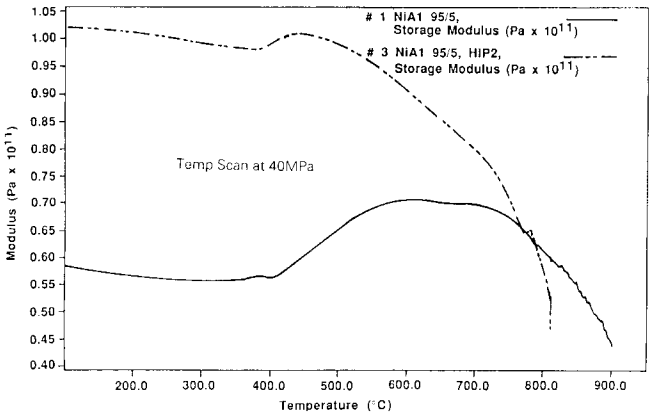

Fig. 5 Mechanical properties of as-sprayed and HIPed Ni-5Al coatings measured using a dynamic mechanical analyzer

form of oxide stringers breaking up into smaller fractions and some degree of grain growth. The extent of oxide disintegration appeared to be related to the temperature and pressure used during the HIP process. Oxide disintegration starts at the free surfaces of the coating and extends to the coating/substrate interface as the HIP temperature increases. The Ni-5Al coatings exhibited a hardness increase in the range of 3.4 to 47%, and Ni-20Al coatings had a hardness increase in the range of 18.5 to 99%. On the other hand, the NiCrAl coatings showed a hardness increase of 3 to 58.9%.

Acknowledgment

The hot isostatic press unit was financed by a Research Grant from the Ministry of Finance (Singapore). The plasma spray

system was financed through Applied Research Fund No. RP 39/89 (Nanyang Technological University). The technical assistance provided by Miss Bernadette Kueh and Miss Yong Mei Yoke is gratefully acknowledged.

References

1. S. Stecura, Effects of Yttrium, Chromium and Aluminum Concentrations in Bond Coatings on the Performance of Zirconia Yttria Thermal Barriers, *Thin Solid Films*, Vol 73, 1980, p 481-489
2. F.J. Dittrich, New Flame Spray Technique for Forming Nickel Aluminide-Ceramic Systems, *Am. Ceram. Soc. Bull.*, Vol 44 (No. 6), 1965, p 492-496
3. S. Sampath, H. Herman, and S. Rangswamy, Ni-Al Revaluated, in *Thermal Spray: Advances in Coatings Technology*, D. Houck, Ed., ASM International, 1987, p 47-53
4. P. Cheang, "The Microstructural and Mechanical Properties of Plasma Sprayed Coatings," Ph.D., Monash University, Dept. of Materials Engineering, Clayton, Australia, 1989
5. P. Cheang and R. McPherson, The Bonding Mechanism of Thermal Sprayed Ni-Al Coating, *J. Inst. Mater. East Asia*, Vol 1, 1992, p 62-68
6. O. Knotek, E. Lugscheider, K.H. Cremer, and W. Rhein, Alumina and Aluminide Formation in Nickel-Aluminium Spraying Powders, *Proc. 9th Int. Thermal Spray Conf.*, 1980, p 281-286
7. C.L. Helgesson, Phase Determination in Flame-Sprayed "Nickel Aluminide" Coating, *Nature*, Vol 209, 1966, p 706-707
8. J.A. Sheppard, Sprayed Coatings of Exothermically Formed Nickel Aluminide, *Br. Weld. J.*, Vol 10 (No. 12), 1963, p 603
9. R. McPherson and P. Cheang, Microstructural Analysis of Ni-Al Plasma Sprayed Coatings, *Proc. 12th Int. Thermal Spray Conf.*, I.A. Bucknow, Ed., The Welding Institute, Cambridge, London, 1990, p 237-246
10. A. Ohmori, C.J. Li, and Y. Arata, The Structure of Plasma Sprayed Coatings Revealed by Copper Electroplating, *Thermal Spray Coatings: Properties, Processes and Applications*, T.F. Bernecki, Ed., ASM International, 1992, p 105-114
11. R. McPherson, The Relationship Between the Mechanism on Formation, Microstructure and Properties, *Thin Solid Films*, Vol 83, 1981, p 297-381
12. H. Kuribayashi, K. Suganuma, Y. Miyamoto, and M. Koizumi, Effects of HIP Treatment on Plasma Sprayed Ceramic Coating onto Stainless Steel, *Am. Ceram. Soc. Bull.*, Vol 65 (No. 9), 1986, p 1306-1310
13. K.A. Khor and N.L. Loh, Hot Isostatic Pressing of Plasma Sprayed Ceramic Coatings, *Ceramics—Adding the Value*, Vol 2, M.J. Bannister, Ed., CSIRO, Melbourne, Australia, 1992, p 804-809
14. H. Ito, R. Nakamura, M. Shiroyama, and T. Sasaki, Post-Treatment of Plasma Sprayed WC-Co Coatings by Hot Isostatic Pressing, *Thermal Spray Research and Applications*, T.F. Bernecki, Ed., ASM International, 1991, p 233-238
15. A.S. Helle, K.E. Easterling, and M.F. Ashby, Hot Isostatic Pressing Diagrams, *Acta Metall.*, Vol 33 (No. 12), 1985, p 2163-2174
16. E. Arzt, M.F. Ashby, and K.E. Easterling, Practical Applications of Hot-Isostatic Pressing Diagrams: Four Case Studies, *Metall. Trans. A*, Vol 14, 1983, p 211-221
17. R.N. Wright, R.L. Williamson, and J.R. Knibloe, Modeling of Hipping Consolidation Applied to Ni_3Al Powders, *Powder Metall.*, Vol 33 (No. 3), 1990, p 253-259